JACS
JOURNAL OF THE AMERICAN CHEMICAL SOCIETY
Communication
pubs.acs.org/JACS

Electron Transfer Dynamics of Iridium Oxide Nanoparticles Attached to Electrodes by Self-Assembled Monolayers

Alessa A. Gambardella,[†] Stephen W. Feldberg,[‡] and Royce W. Murray*[,†]

[†]Kenan Laboratories of Chemistry, University of North Carolina, Chapel Hill, North Carolina 27599, United States
[‡]Chemistry Department, Brookhaven National Laboratory, Upton, New York 11973, United States

Supporting Information

ABSTRACT: Self-assembled monolayers (SAMs) of carboxylated alkanethiolates ($-S(CH_2)_{n-1}CO_2^-$) on flat gold electrode surfaces are used to tether small (ca. 2 nm d.) iridium(IV) oxide nanoparticles ($Ir^{IV}O_X$ NPs) to the electrode. Peak potential separations in cyclic voltammetry (CV) of the nanoparticle $Ir^{IV/III}$ wave, in pH 13 aqueous base, increase with n, showing that the $Ir^{IV/III}$ apparent electron transfer kinetics of metal oxide sites in the nanoparticles respond to the imposed SAM electron transfer tunneling barrier. Estimated apparent electron transfer rate constants (k_{app}^0) for n = 12 and 16 are 9.8 and 0.12 s^{-1}. Owing to uncompensated solution resistance, k_{app}^0 for n = 8 was too large to measure in the potential sweep experiment. For the cathodic scans, coulometric charges under the $Ir^{IV/III}$ voltammetric waves were independent of potential scan rate, suggesting participation of all of the iridium oxide redox sites (ca. 130 per NP) in the NPs. These experiments show that it is possible to control and study electron transfer dynamics of electroactive nanoparticles including, as shown by preliminary experiments, that of the electrocatalysis of water oxidation by iridium oxide nanoparticles.

There is a substantial literature on the electrochemistry and electron transfer kinetics of redox species attached by self-assembled monolayers (SAMs)[1] to planar gold and Au nanoparticle surfaces. Attaching nanoparticles (NPs) to planar surfaces using SAMs, however, has received little attention,[2] and there have been no previous measurements of electron transfer dynamics of electroactive NPs on SAMs. This paper describes the cyclic voltammetry (CV) of ca. 2 nm diameter (d.) iridium(IV) oxide nanoparticles ($Ir^{IV}O_X$ NPs)[3,4] attached by SAMs to Au electrode surfaces, and the determination of apparent $Ir^{IV/III}$ electron transfer rate constants of the NP sites. Electron transfer rates of SAM-attached small molecule redox species (such as ferrocene) are known[1f−k] to depend on the lengths of the alkane spacers linking them to the electrode surface. We demonstrate here an analogous linker chain length dependence for kinetics of the $Ir^{IV/III}O_X$ NP reaction and additionally for the electrocatalyzed water oxidation[3,5,6] by a higher oxidation state of this metal oxide NP.

Surface-attachment of the $Ir^{IV}O_X$ NPs was effected by exposing carboxylate-terminated SAMs to basic (pH 13) $Ir^{IV}O_X$ NP solutions. (See cartoon structure in Figure 1 and Supporting Information.) The SAMs comprised entirely 16-mercaptohexadecanoic acid (C16), 12-mercaptododecanoic acid (C12), or 8-mercaptooctanoic acid (C8). Assemblies of $Ir^{IV}O_X$ NPs thusly attached to SAM coated Au surfaces are referred to as NP-SAMs. Cyclic voltammetry of the $Ir^{IV/III}$ redox wave of $Ir^{IV}O_X$ NPs captured by SAMs of these three chain lengths is illustrated in Figure 1. The NP-SAM voltammetry (in NP-free electrolyte solution) is quite stable over many cyclical potential scans. The stability is degraded (as expected[1d,7]) by scans to potentials sufficiently negative as to promote thiol desorption or sufficiently positive to effect Au oxide formation. The coverage of attached NPs was measured from the charge under the $Ir^{IV/III}$ wave, which was independent of potential scan rate (v) from 0.1 to 10 V/s (Table S-1). The obtained coverage (Γ_{IrO2}) varied from a small fraction to a nearly complete monolayer of NPs (theoretical coverage is estimated as ca. 4×10^{-11} mol NP/cm^2 or 5×10^{-9} mol Ir/cm^2 for ca. 2 nm d. NPs containing ~130 Ir sites each). Owing in part to the SAM's suppression of double layer capacitance currents, the $Ir^{IV/III}$ redox wave is well-defined at both 10% (e.g., 4×10^{-12} mol NP/cm^2) and ca. 1% (e.g., 4×10^{-13} mol NP/cm^2) coverage of NPs on the SAM.

Figure 1 shows that the separations between oxidation and reduction $Ir^{IV/III}$ peak potentials (ΔE_{PEAK}) increase with SAM chain length at a given scan rate, ν. This effect, reflecting influence of chain length on apparent electron transfer rates, is strong evidence that the NPs are attached to the SAM carboxylate termini, as opposed to being adsorbed to the Au electrode surface. The suppressed double layer charging currents also show that the SAMs survive exposure to aqueous base during the NP-SAM preparation (Figure S-1).

Unsurprisingly, $Ir^{IV}O_X$ NPs also adsorb directly to naked (no SAM) Au surfaces as indicated by appearance of the $Ir^{IV/III}$ NP wave (and a nonsuppressed double layer current background) after exposure to a NP solution. These adsorbed NPs exhibit ΔE_{PEAK} values that are very similar to those of C8 NP-SAMs (Figure S-2), because both are dominated by solution uncompensated resistances. The NP adsorption (and associated $Ir^{IV/III}$ NP voltammetry) is, however, entirely quenched if the electrode is coated with a nonfunctionalized alkanethiolate SAM before exposure to the NP solution. This "direct" adsorption does not appear to contribute to the CV responses in Figure 1.

An interesting aspect of the NP $Ir^{IV/III}$ formal potentials, $E^{\circ\prime}$, is that values for NP-SAMs, $E^{\circ\prime} \sim -0.40$ V versus Ag/AgCl, lie between those of freely diffusing $Ir^{IV}O_X$ NPs ($E^{\circ\prime} \sim -0.63$ V, again at pH 13)[5] and those of $Ir^{IV}O_X$ NPs in electroflocculated

Received: February 6, 2012
Published: March 21, 2012

dx.doi.org/10.1021/ja301212r | J. Am. Chem. Soc. 2012, 134, 5774−5777

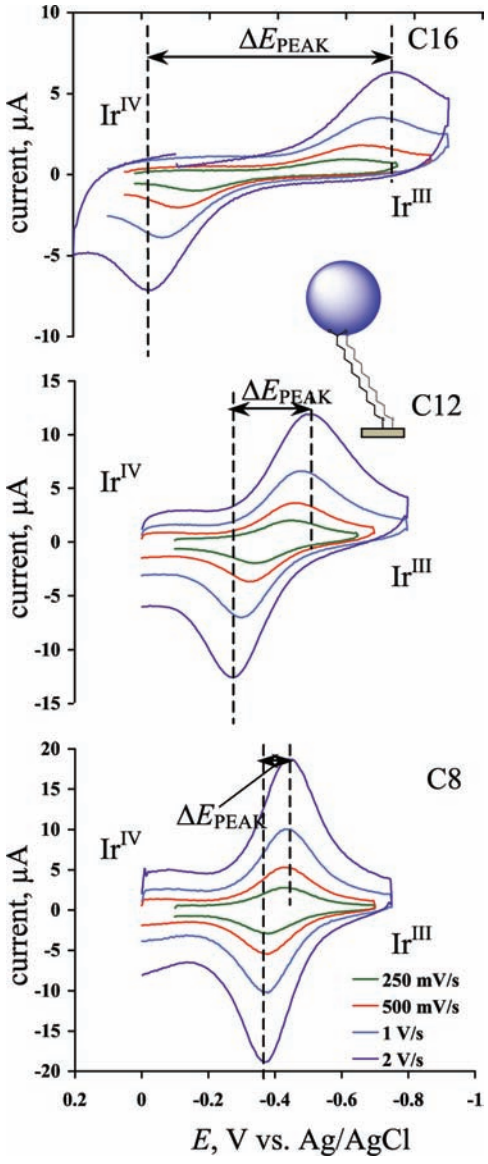

Figure 1. Cyclic voltammetry (CV) of the $Ir^{IV/III}$ redox couple for NPs immobilized on SAMs (see cartoon at center) of C16, C12, and C8 illustrating ΔE_{PEAK} dependence on chain length. Potential scan rates are 250 mV/s, 500 mV/s, 1 V/s, and 2 V/s. CVs were performed in 1.0 M electrolyte (1:9 mol ratio of $NaOH/KNO_3$, pH ~13) with 0.106 cm^2 area electrode. See Table S-1 for surface coverage, Γ_{IrO2}.

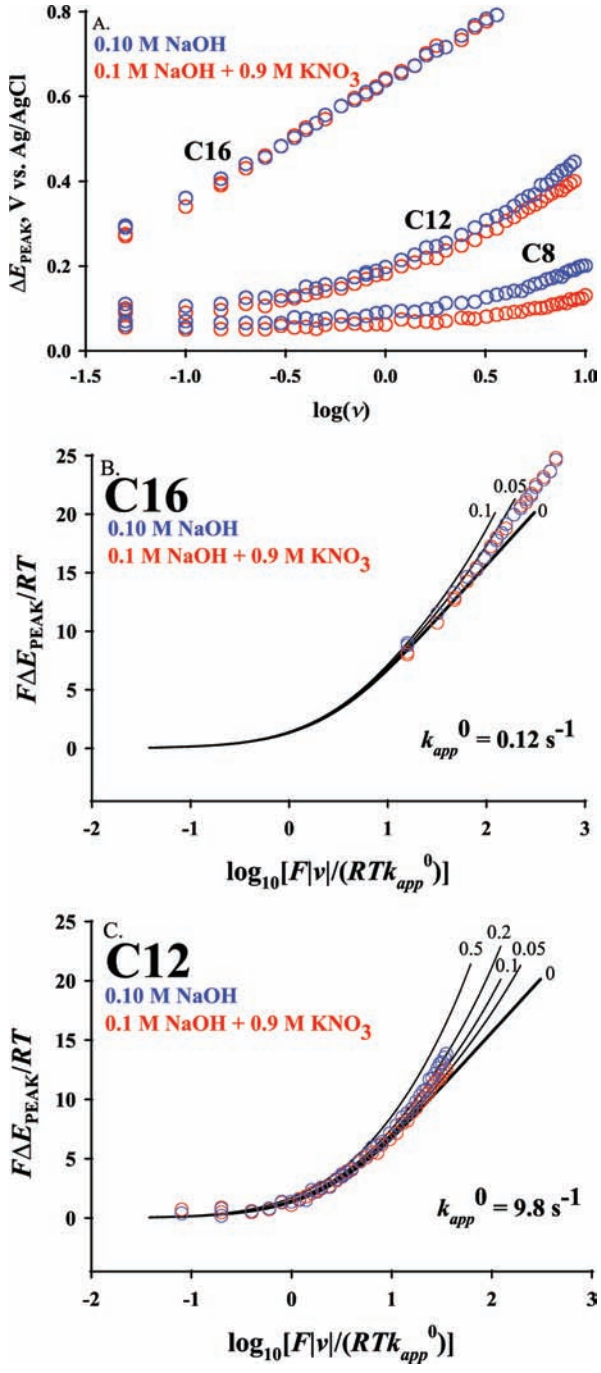

Figure 2. (A) Experimental data for C16, C12, and C8 NP-SAMs from CVs performed in 0.1 M NaOH electrolyte (blue) and 1.0 M electrolyte (1:9 mol ratio of $NaOH/KNO_3$, pH ~13) (red). (B,C) Dependence of normalized experimental ΔE_{PEAK} on SAM chain length and potential scan rate ν, and comparison to predictions of Butler–Volmer electron transfer theory and uncompensated solution resistance effect (solid lines). k_{app}^0 = 9.8 and 0.12 s^{-1} for C12 and C16 NP-SAMs, respectively, from best-fit match. Γ_{IrO2}'s are ~1.2×10^{-10} and ~4.5×10^{-11} mol Ir/cm^2, respectively. The numerical labels on theoretical curves denote different choices of the normalized resistance parameter $R_{UNC,norm}$ = (area) $F^2 k_{app}^0 \Gamma_{IrO2} R_{UNC}/RT$. R_{UNC} is the uncompensated resistance. Double layer capacitance is assumed to be negligible.

films ($E^{\circ\prime}$ ~ −0.25 V).[3] Indeed, the SAM-bound NPs exist in an intermediate environment, being both held to a surface by the SAM and exposed to the overlying electrolyte solution.

The difference between the peak potentials of oxidation and reduction waves for immobilized species (ΔE_{PEAK}) is ideally zero for a reversible reaction,[8] and increases when the apparent electron transfer kinetics (k_{app}^0) are slow or potential scan rate is increased. As noted above, Figure 1 shows that increasing the SAM chain length substantially enlarges the ΔE_{PEAK} values at a given ν, signaling depression of apparent electron transfer rates of the NP $Ir^{IV/III}$ reactions by the SAM chain electron tunneling barrier. The peak potential separations increase with increased ν, which provides an avenue for determining the NP $Ir^{IV/III}$ apparent reaction rate constants.

Figure 2A (enlarged in Figure S-3) shows plots of ΔE_{PEAK} versus log ν for the C16, C12, and C8 systems obtained at pH 13 at two different ionic strengths associated with 0.1 M NaOH (blue open circles) and 0.1 M NaOH + 0.9 M KNO_3 (red open circles). A number of important conclusions can be reached by inspection:

dx.doi.org/10.1021/ja301212r | J. Am. Chem. Soc. 2012, 134, 5774−5777

1. The data for C16 and C12 are virtually unaffected by the difference in ionic strength because k_{app}^{0} is small, v is small, and, for the extant ionic strengths, iR_{UNC} is quite small.

2. The data for C8 are significantly affected by the difference in ionic strength because the k_{app}^{0} associated with the shorter C8 tether v is larger, the currents associated with the larger scan rates are larger, and the ΔE_{PEAK} is very much a function of iR_{UNC}.

3. The log of the ratio of the apparent rate constants—$k^0_{app,C12}$ and $k^0_{app,C16}$ for C12 and C16, respectively— is roughly approximated by the lateral shift of the plots, ~1.8 $\log_{10}$ units, and therefore, $k^0_{app,C12}/k^0_{app,C16}$~60.

4. One feature of the data, most apparent for the C12 and C8 data, is that ΔE_{PEAK} does not go to zero at low potential scan rates, perhaps indicative of a structural change associated with the redox process, which is not uncommon when intercalation (of ions in this case) is involved.[9] (The structural change that appears to accompany the $Ir^{IV/III}$ transformation effects hysteresis and an energy loss. There does not appear to be a significant dependence of this hysteresis on the ionic strength or on the tether (C12 or C16).) Note that the limiting value of ΔE_{PEAK} for small v ($\Delta E_{PEAK,baseline}$) does not exhibit significant dependence on the ionic strength. In the absence of any good theory to deal with the suggested structure change, the aforementioned "offset" is corrected by the simple expedient of adjusting the $\Delta E_{PEAK,baseline}$ to optimize the fit.

A preliminary attempt to develop theory correlating ΔE_{PEAK}, k_{app}^{0}, R_{UNC}, and v invoked the simplifying assumption that electron transfer kinetics can be adequately described by Butler–Volmer theory with a transfer coefficient, α, of 0.5 (Figure S-4) and a one-electron transfer.[8] It is possible that Marcusian effects come into play with increasing values of ΔE_{PEAK}.[1k] The theory differs from that given by Laviron[10] in that we focus on ΔE_{PEAK} and include the effects of R_{UNC}. Relevant working curves, computed numerically (Supporting Information), were plotted as $F\Delta E_{PEAK}/RT$ versus $\log_{10}[Fv/RTk_{app}^{0}]$ as a function of the dimensionless resistance, $R_{UNC,norm} = (\text{area})F^2k_{app}^{0}\Gamma_{IrO2}R_{UNC}/RT$.

Analyses of the data in Figure 2A are shown in Figure 2B,C. The resultant values for the apparent rate constants for C16 and C12 NP-SAMs are 0.12 and 9.8 s^{-1}, respectively. The electron transfer rate of ferrocene on $-S(CH_2)_{16}CO_2^-$ has been reported by Chidsey[1k] as 1.3 s^{-1} while that of cytochrome C covalently immobilized on $-S(CH_2)_{15}CO_2^-$ has been reported by Tarlov[11] and co-workers as ca. 1 s^{-1}. Of course, the chemical identities of these earlier examples are not easily compared to the NP-SAMs.

As already noted, data for C8 NP-SAMs, on the other hand, were found to be dominated by R_{UNC} effects (i.e., k_{app}^{0} is too large to be measured by the CV protocol), as shown in Figure S-5, and thus, are devoid of useful electron transfer kinetic information.

There are a number of richly interesting issues that invite further study of this novel mode of electron transfer rate control for NPs. First and importantly, we note that the $Ir^{IV/III}O_X$ reaction is a one electron-one proton process,[4] so the NP-SAMs give access to a possible case of proton-coupled electron transfer (PCET)[11] in which the rate of the electron transfer component can be profitably manipulated. Second, there may be multiple carboxylate attachments to each NP (see cartoon in Figure 1 or Scheme 1 of Supporting Information). This possibility can be assessed by dilution of the SAM carboxylate sites with nonbinding SAM chains. The electron transfer rate constants k_{app}^{0} accordingly have been labeled *apparent* values. Third, use of SAMs with an expanded variety of SAM chain lengths will aid further explorations (but will also require a synthetic effort). Fourth, a change of the experimental approach, such as toward potential step[1h,i,k] assessments of k_{app}^{0}, and use of smaller electrodes (to lessen uncompensated resistance effects) should give access to better kinetic data for the shorter chain lengths. This step will also allow examination of consequences, if any, of the somewhat broadened and differing cathodic–anodic peak shapes of the $Ir^{IV/III}O_X$ voltammetry. The full-width-half-maximum of the peaks for the C12 and C16 systems is wider than ideal for a 1-electron transfer. This could be caused by nonuniformity of NP sizes, size-dependent $E^{o\prime}$ values, variations in the mode of attachment of the NP to the SAM, and/or by some other nonideal behavior.[12]

The results presented here suggest possibilities for exploration of electron transfer rate control of the electrocatalytic oxidation of water by the $Ir^{IV}O_X$ NPs in higher valent states. Preliminary results (Figure 3) are highly promising. A strong

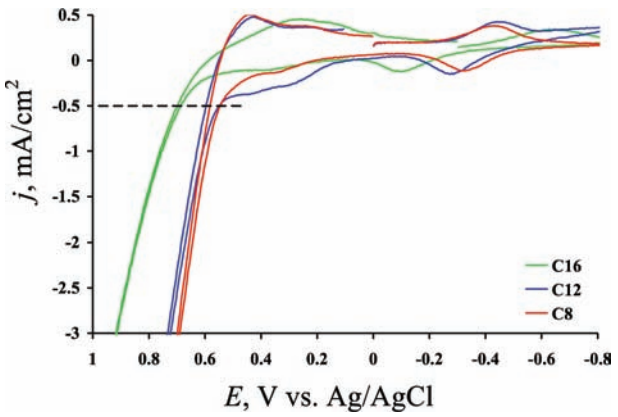

Figure 3. Cyclic voltammetry (CV) of NPs immobilized on C16, C12, and C8 SAMs. The large currents at positive potentials correspond to electrocatalyzed water oxidation, which occurs at increasing overpotential with increasing SAM chain length. CVs were performed at 500 mV/s in 0.1 M NaOH (pH ~13) electrolyte with 0.106 cm^2 electrode area. Surface coverage, Γ_{IrO2}, was ~1.2×10^{-9}, 1.1×10^{-9}, and 1.0×10^{-9} mol Ir/cm^2 for C16, C12, and C8 SAMs, respectively. The dotted line at 0.5 mA/cm^2 marks C16, C12, and C8 potentials for catalysis of water oxidation at 0.68, 0.55, and 0.546 V, respectively. With repeated scans, the NP-SAM becomes degraded by Au oxide formation.

increase in oxidation currents is seen at positive potentials, which are known[3,5,6] to reflect high-valent NP electrocatalysis of water oxidation. In a rotated ring-disk electrode experiment[3] in which the disk was $Ir^{IV}O_X$ NP-SAM-coated, O_2 was detected at the ring.[13] The significant aspect of Figure 3 is that the water oxidation process *becomes shifted to more positive potentials as the NP-SAM chain length is increased*, signaling a SAM-imposed kinetic control of the reaction. The potentials for water oxidation at 0.5 mA/cm^2 are 0.546, 0.55, and 0.68 V for C8, C12, and C16 SAMs, respectively. For comparison, the potential for water oxidation by electroflocculated[14] $Ir^{IV}O_X$ NP films is 0.50 V.[3] The unmistakable retarding effect of NP-SAM chain length in Figure 3 opens a potential avenue to studying the water oxidation reaction mechanism at manipulable reaction rates. Varying the chain length of NP-SAM assemblies also provides a model for understanding the role of electron transfer

dx.doi.org/10.1021/ja301212r | J. Am. Chem. Soc. 2012, 134, 5774–5777

rates in other water oxidation immobilized-catalyst schemes found in the literature,[15] and other electrocatalyzed reactions.

■ ASSOCIATED CONTENT

Supporting Information

Experimental procedure, theoretical discussion, detailed CV results, control CV data, and coverage determination. This material is available free of charge via the Internet at http://pubs.acs.org.

■ AUTHOR INFORMATION

Corresponding Author

rwm@unc.edu

Notes

The authors declare no competing financial interest.

■ ACKNOWLEDGMENTS

This work was supported in part (theory and consultation by S.W.F.) by an award from NSF (CHE-0950320) and in part by the UNC EFRC: Center for Solar Fuels, an Energy Frontier Research Center funded by the U.S. Department of Energy, Office of Science, Office of Basic Energy Sciences under Award Number DE-SC0001011, supporting A.A.G. A.A.G acknowledges a graduate research fellowship from the Eastman Chemical Company (Kingsport, TN) for summer of 2011.

■ REFERENCES

(1) (a) Love, J. C.; Estroff, L. A.; Kriebel, J. K.; Nuzzo, R. G.; Whitesides, G. M. *Chem. Rev.* **2005**, *105*, 1103. (b) Bain, C. D.; Troughton, E. B.; Tao, Y.-T.; Evall, J.; Whitesides, G. M.; Nuzzo, R. G. *J. Am. Chem. Soc.* **1989**, *111*, 321. (c) Eckermann, A. L.; Feld, D. J.; Shaw, J. A.; Meade, T. J. *Coord. Chem. Rev.* **2010**, *254*, 1769. (d) Vericat, C.; Vela, M. E.; Benitez, G.; Carro, P.; Salvarezza, R. C. *Chem. Soc. Rev.* **2010**, *39*, 1805. (e) Ulman, A. *Chem. Rev.* **1996**, *96*, 1533. (f) Kasmi, A. E.; Wallace, J. M.; Bowden, E. F.; Binet, S. M.; Linderman, R. J. *J. Am. Chem. Soc.* **1998**, *120*, 225. (g) Liu, B.; Bard, A. J.; Mirkin, M. V.; Creager, S. E. *J. Am. Chem. Soc.* **2004**, *126*, 1485. (h) Smalley, J. F.; Sachs, S. B.; Chidsey, C. E. D.; Dudek, S. P.; Sikes, H. D.; Creager, S. E.; Yu, C. J.; Feldberg, S. W.; Newton, M. D. *J. Am. Chem. Soc.* **2004**, *126*, 14623. (i) Smalley, J. F.; Finklea, H. O.; Chidsey, C. E. D.; Linford, M. R.; Creager, S. E.; Ferraris, J. P.; Chalfant, K.; Zawodzinsk, T.; Feldberg, S. W.; Newton, M. D. *J. Am. Chem. Soc.* **2003**, *125*, 2004. (j) Smalley, J. F.; Feldberg, S. W.; Chidsey, C. E. D.; Linford, M. R.; Newton, M. D.; Liu, Y.-P. *J. Phys. Chem.* **1995**, *99*, 13141. (k) Chidsey, C. E. D. *Science* **1991**, *251*, 919. (l) Collinson, M.; Bowden, E. F; Tarlov, M. J. *Langmuir* **1992**, *8*, 1247.

(2) (a) Chen, S.; Deng, F. *Proc. SPIE* **2002**, *4807*, 93. (b) Chen, S. *J. Phys. Chem. B.* **2000**, *104*, 663. (c) Peng, Z.; Qu, Z.; Dong, S. *Langmuir* **2004**, *20*, 5. (d) Chan, E. W. L.; Yu, L. *Langmuir* **2002**, *18*, 311. (e) Malinsky, M. D.; Kelly, K. L.; Schatz, G. C.; Van Duyne, R. P. *J. Am. Chem. Soc.* **2001**, *123*, 1471. (f) Sheibley, D.; Tognarelli, D. J.; Szymanik, R.; Leopold, M. C. *J. Mater. Chem.* **2005**, *15*, 491. (g) Sardar, R.; Beasley, C. A.; Murray, R. W. *Anal. Chem.* **2009**, *81*, 6960.

(3) Nakagawa, T.; Beasley, C. A.; Murray, R. W. *J. Phys. Chem. C.* **2009**, *113*, 12958.

(4) Gambardella, A. A.; Bjorge, N. S.; Alspaugh, V. K.; Murray, R. W. *J. Phys. Chem. B.* **2011**, *115*, 21659.

(5) Nakagawa, T.; Bjorge, N. S.; Murray, R. W. *J. Am. Chem. Soc.* **2009**, *131*, 15578.

(6) Yagi, M.; Tomita, E.; Sakita, S.; Kuwabara, T.; Nagai, K. *J. Phys. Chem. B.* **2005**, *109*, 21489.

(7) (a) Kondo, T.; Sumi, T.; Uosaki, K. *J. Electroanal. Chem.* **2002**, *538*, 59. (b) Zhong, C.-J.; Porter, M. D. *J. Electroanal. Chem.* **1997**, *425*, 147. (c) Weisshaar, D. E.; Lamp, B. D.; Porter, M. D. *J. Am. Chem. Soc.* **1992**, *114*, 5860. (d) Widrig, C. A.; Chung, C.; Porter, M. D. *J. Electroanal. Chem.* **1991**, *310*, 335.

(8) Bard, A. J.; Faulkner, L. R. *Electrochemical Methods: Fundamentals and Applications*, 2nd ed.; John Wiley & Sons, Inc.: New York, 2001; pp 96 and 591.

(9) Feldberg, S. W.; Rubinstein, I. *J. Electroanal. Chem.* **1988**, *240*, 1.

(10) Laviron, E. *J. Electroanal. Chem.* **1979**, *101*, 19.

(11) (a) Madhiri, N.; Finklea, H. O. *Langmuir* **2006**, *22*, 10643. (b) Haddox, R. M.; Finklea, H. O. *J. Phys. Chem. B.* **2004**, *108*, 1694. (c) Haddox, R. M.; Finklea, H. O. *J. Electroanal. Chem.* **2003**, *550–551*, 351. (d) Murgida, D. H.; Hildebrandt, P. *J. Am. Chem. Soc.* **2001**, *123*, 4062. (e) Zhang, W.; Rosendahl, S. M.; Burgess, I. J. *J. Phys. Chem. C.* **2010**, *114*, 2738. (f) Zhang, W.; Burgess, I. J. *Phys. Chem. Chem. Phys.* **2010**, *13*, 2151. (g) Haga, M.; Hong, H.-G.; Shiozawa, Y.; Kawata, Y.; Monjushiro, H.; Fukuo, T.; Arakawa, R. *Inorg. Chem.* **2000**, *39*, 4566. (h) Lemmer, C.; Bouvet, M.; Meunier-Prest, R. *Phys. Chem. Chem. Phys.* **2011**, *13*, 13327. (i) Ludlow, M. K.; Soudackov, A. V.; Hammes-Schiffer, S. *J. Am. Chem. Soc.* **2010**, *132*, 1234. (j) Abhayawardhana, A. D.; Sutherland, T. C. *J. Phys. Chem. C.* **2009**, *113*, 4915.

(12) Clark, R. A.; Bowden, E. F. *Langmuir* **1997**, *13*, 559.

(13) Gambardella, A. A.; Murray, R. W. Unpublished results, UNC, Fall, 2011.

(14) To allow comparison, the values reported are at the current density used in previous reports. (Ref 3.)

(15) (a) Youngblood, W. J.; Lee, S.-H. A.; Kobayashi, Y.; Hernandez-Pagan, E. A.; Hoertz, P. G.; Moore, T. A.; Moore, A. L.; Gust, D.; Mallouk, T. E. *J. Am. Chem. Soc.* **2009**, *131*, 926. (b) Youngblood, W. J.; Lee, S.-H. A.; Maeda, K.; Mallouk, T. E. *Acc. Chem. Res.* **2009**, *42*, 1966.